

Alma Mater Studiorum Università di Bologna  
Archivio istituzionale della ricerca

Crosslinked polytriazole membranes for organophilic filtration

This is the final peer-reviewed author's accepted manuscript (postprint) of the following publication:

*Published Version:*

Chisca, S., Falca, G., Musteata, V.E., Boi, C., Nunes, S.P. (2017). Crosslinked polytriazole membranes for organophilic filtration. JOURNAL OF MEMBRANE SCIENCE, 528, 264-272 [10.1016/j.memsci.2016.12.060].

*Availability:*

This version is available at: <https://hdl.handle.net/11585/576740> since: 2017-05-15

*Published:*

DOI: <http://doi.org/10.1016/j.memsci.2016.12.060>

*Terms of use:*

Some rights reserved. The terms and conditions for the reuse of this version of the manuscript are specified in the publishing policy. For all terms of use and more information see the publisher's website.

This item was downloaded from IRIS Università di Bologna (<https://cris.unibo.it/>).  
When citing, please refer to the published version.

(Article begins on next page)



جامعة الملك عبد الله  
للعلوم والتقنية  
King Abdullah University of  
Science and Technology

## Crosslinked polytriazole membranes for organophilic filtration

Item Type	Article
Authors	Chisca, Stefan; Falca, Gheorghe; Musteata, Valentina-Elena; Boi, Cristiana; Nunes, Suzana Pereira
Citation	Chisca S, Falca G, Musteata VE, Boi C, Nunes SP (2016) Crosslinked polytriazole membranes for organophilic filtration. Journal of Membrane Science. Available: <a href="http://dx.doi.org/10.1016/j.memsci.2016.12.060">http://dx.doi.org/10.1016/j.memsci.2016.12.060</a> .
Eprint version	Post-print
DOI	<a href="https://doi.org/10.1016/j.memsci.2016.12.060">10.1016/j.memsci.2016.12.060</a>
Publisher	Elsevier BV
Journal	Journal of Membrane Science
Rights	NOTICE: this is the author's version of a work that was accepted for publication in Journal of Membrane Science. Changes resulting from the publishing process, such as peer review, editing, corrections, structural formatting, and other quality control mechanisms may not be reflected in this document. Changes may have been made to this work since it was submitted for publication. A definitive version was subsequently published in Journal of Membrane Science, 30 December 2016. DOI: <a href="https://doi.org/10.1016/j.memsci.2016.12.060">10.1016/j.memsci.2016.12.060</a>
Download date	17/05/2022 14:53:13
Link to Item	<a href="http://hdl.handle.net/10754/622619">http://hdl.handle.net/10754/622619</a>

Crosslinked polytriazole membranes for  
organophilic filtration

Stefan Chisca, Gheorghe Falca, Valentina Elena  
Musteata, Cristiana Boi, Suzana P. Nunes



PII: S0376-7388(16)31952-4  
DOI: <http://dx.doi.org/10.1016/j.memsci.2016.12.060>  
Reference: MEMSCI14985

To appear in: *Journal of Membrane Science*

Received date: 16 October 2016  
Revised date: 14 December 2016  
Accepted date: 29 December 2016

Cite this article as: Stefan Chisca, Gheorghe Falca, Valentina Elena Musteata Cristiana Boi and Suzana P. Nunes, Crosslinked polytriazole membranes for organophilic filtration, *Journal of Membrane Science* <http://dx.doi.org/10.1016/j.memsci.2016.12.060>

This is a PDF file of an unedited manuscript that has been accepted for publication. As a service to our customers we are providing this early version of the manuscript. The manuscript will undergo copyediting, typesetting, and review of the resulting galley proof before it is published in its final citable form. Please note that during the production process errors may be discovered which could affect the content, and all legal disclaimers that apply to the journal pertain.

# Crosslinked polytriazole membranes for organophilic filtration

Stefan Chisca<sup>1</sup>, Gheorghe Falca<sup>1,2</sup>, Valentina Elena Musteata<sup>1</sup>, Cristiana Boi<sup>2</sup>, Suzana P. Nunes<sup>1\*</sup>

<sup>1</sup>King Abdullah University of Science and Technology (KAUST), Biological and Environmental Science and Engineering Division (BESE), Thuwal, 23955-6900, Saudi Arabia

<sup>2</sup>Dipartimento di Ingegneria Civile, Chimica, Ambientale e dei Materiali, DICAM, Università di Bologna, via Terracini 28, 40131 Bologna, Italy

\*Corresponding author. Prof. Suzana P. Nunes. Tel.: +966 544700052;

suzana.nunes@kaust.edu.sa

## Abstract

We report the preparation of crosslinked membranes for organophilic filtration, by reacting a new polytriazole with free OH groups, using non-toxic poly (ethylene glycol) diglycidyl ether (PEGDE). The OH-functionalized polymer was obtained by converting the oxadiazole to triazole rings with high yield (98%). The maximum degree of crosslinking is achieved after 6 h of reaction. The crosslinked polytriazole membranes are stable in a wide range of organic solvents and show high creep recovery, indicating the robustness of crosslinked membranes. The influence of different casting solutions and different crosslinking time on the membrane morphology and membrane performance was investigated. The membranes performance was studied in dimethylformamide (DMF) and (tetrahydrofuran) THF. We achieved a permeance for THF of  $49 \text{ L m}^{-2} \text{ h}^{-1} \text{ bar}^{-1}$  for membranes with molecular weight cut off (MWCO) of  $7 \text{ kg mol}^{-1}$  and a permeance for THF of  $17.5 \text{ L m}^{-2} \text{ h}^{-1} \text{ bar}^{-1}$  for membranes with

MWCO of 3 kg mol<sup>-1</sup>. Our data indicate that by using the new polytriazole is possible to adjust the pore dimensions of the membranes to have a MWCO, which covers ultra- and nanofiltration range.

**Keywords:** polytriazole, crosslinked membrane, high creep resistance, solvent resistance

## 1. Introduction

Many reactions in the chemical, pharmaceutical and petrochemical industries do not yield pure products, requiring additional separation processes. Large amount of organic solvents is frequently generated and needs to be recovered for further use. Conventional separation methods involve high energy consumption and membrane technology could be a competitive energy saving alternative process [1-3].

The main challenge of this technology is to design membranes which are easy to process by common techniques and are stable in a wide range of pH and organic solvents. Although inorganic membranes offer high stability in organic solvents, their cost, more difficult processability for manufacture and integration in modules and mechanical stability are factors, which make them less attractive than polymeric membranes [4]. Inorganic materials incorporated in polymer matrix have been explored as mixed matrix to combine properties of both materials classes for filtration in organic solvents [5-8]. An example of growing interest is the incorporation of metal organic frameworks in thin film composite membranes to improve their performance [9-10].

The most used polymers for the manufacture of membranes for organic solvent nanofiltration (OSN) are crosslinked polyimides, due to their relatively easy synthesis and high

stability in solvents. However, the imide ring is not stable in high concentration of organic and inorganic bases [11]. Polysulfone and perfluorinated polymers (polyvinylidene fluoride and polytetrafluoroethylene) have been reported to be stable in the whole pH range, but are soluble in strong organic solvents [12-15]. Crosslinked polybenzimidazole is stable in a wide range of pH and organic solvents, but the processability of polybenzimidazole in common solvents is relatively difficult [16, 17]. Recently, poly (ether ether ketone) has been reported as an alternative material for OSN due to the high chemical resistance in harsh solvents, without requiring a crosslinking step, using strong acids for membrane preparation [18, 19]. Polyoxadiazole has been reported by our group for OSN membranes, without need for crosslinking but also requiring acids for dissolution [20]. Both poly (ether ether ketone) and the reported polyoxadiazole membranes are stable in several organic solvents. However they were prepared with casting solutions based on sulphuric acid or in a mixture of methane sulphonic acid and sulphuric acid, which require additional safety precautions [18-20]. Therefore, more polymeric structures should be developed to combine the easy processability by conventional industrial methods with stability in a wide range of organic solvents. Polybenzoxazole membranes prepared by thermal rearrangement from polyimide precursors have been successfully explored for gas separation or fuel cell [21, 22]. Our group has been investigating fluorinated polyoxadiazoles and sulfonated polytriazoles prepared by polycondensation for fuel cell application [23-25] using one-pot polycondensation reactions. We recently reported the direct synthesis of a hydroxyl-functionalized copolyazole, from fluorinated oxadiazole monomers [26]. The polytriazole is soluble in organic solvents and easy to process. After crosslinking the obtained membranes were stable in several solvents. A weak point was,

however, the crosslinking segment: the membrane was not stable in a broad pH range due to the presence of silane groups, which are sensitive to basic media [26].

Here we report the facile synthesis of new crosslinked polytriazole membranes for organophilic filtration by using poly(ethylene glycol) diglycidyl ether (PEGDE) as crosslinker, which is non-toxic and non-expensive. The resulting membranes are stable in wide range of organic solvents and in all pH range. Without crosslinking, polytriazole is highly soluble in organic solvents, since 98% of the monomeric units are functionalized with free OH groups. The same OH groups are excellent sites for post crosslinking.

## 2. Experimental part

### 2.1. Materials and methods

4-Aminophenol, poly(ethylene glycol) diglycidyl ether (PEGDE) ( $M_n$  500), tetrahydrofuran (THF), N,N'-dimethylformamide (DMF), N,N-dimethylacetamide (DMAc), dimethyl sulfoxide (DMSO), N-methyl-2-pyrrolidone (NMP), polyphosphoric acid (PPA), polystyrene (PS), poly(ethylene glycol) (PEG) and all other reagents were purchased from Sigma-Aldrich. The polyoxadiazole precursor was synthesized in our lab by polycondensation reaction [23, 24]. All chemicals were used as received.

### 2.2. Synthesis of polytriazole (PTA-OH)

Polytriazole with OH groups was synthesized following a method analogous to that previously described by our group [26], but optimized to have 98% OH functionalization. In a typical procedure, 50 g (0.135 mol) of polyoxadiazole precursor were added to a 2000 ml three neck flask and were dissolved in 333 ml NMP. After the polyoxadiazole precursor was

dissolved, 2 g of PPA and 37 g (0.3378 mol) of 4-aminiphenol were added and then the reaction mixture was heated to 195 °C in nitrogen atmosphere for 15 h. The resulting solution was precipitated in a mixture of water-methanol at 60°C and purified by re-precipitation from NMP. The polymer was dried in a vacuum oven at 110°C (yield 48 g, 84%, based on the repeat unit).

FTIR: 3000 – 3500  $\text{cm}^{-1}$  (OH groups), 1518  $\text{cm}^{-1}$  (triazole ring).

$^1\text{H}$  NMR (400 MHz; DMF- $d_7$ ):  $\delta$  ppm 10.45 (s, 1H), 7.71 (d, 4H), 7.44-7.42 (m, 6H), 7.00 (d, 2H).  $^{13}\text{C}$  NMR (400 MHz; DMF- $d_7$ ):  $\delta$  ppm 159.7, 154.3, 133.8, 130.3, 129.9, 129.1, 128.6, 126.3, 125.8, 122.9, 120.1, 116.9, 64.8, 64.5, 64.3.

### 2.3. Synthesis of crosslinked polytriazole membranes

The polytriazole membranes were obtained by phase inversion [27, 28]. We used two different casting solutions: (i) 18 wt% polytriazole (PTA-OH) in NMP, and (ii) 18 wt% PTA-OH in a 9/1 mixture of NMP/THF. The polymer solutions were cast on a glass plate using a doctor blade with 100  $\mu\text{m}$  gap. The polymer membranes were obtained by immersing the glass plate in water. They were kept in water for 24 h to eliminate any remaining solvent. The second solution was used to study the influence of the evaporation time on the pore size. After the polymer solution was cast on the glass plate the solvent was evaporated for 0 s, 10 s, and 30 s before immersion in the water bath. The incipient membranes were submerged in 10 wt% poly(ethylene glycol) diglycidyl ether (PEGDE) aqueous solution at 80°C for 3, 6 and 9 h. After the crosslinking reaction all membranes were washed with water and a mixture of water – methanol.

### 2.4 Characterization



The success of the polytriazole synthesis was evaluated by Nuclear Magnetic Resonance (NMR) Spectroscopy. The samples were dissolved in DMF- $d_7$  and the spectra recorded on Bruker Advance III 600 spectrometer. The structures of polytriazole and the crosslinked membrane were evaluated by Fourier Transform Infrared Spectroscopy (FTIR). The FTIR spectra were recorded by performing 16 scans with a spectral resolution of  $4\text{ cm}^{-1}$ , at room temperature, on a Nicolet 6700 FT-IR System with Continuum IR Microscope.

The thermal stability of the membranes was evaluated by thermogravimetric analysis (TGA) on a TGA Q50 by TA instruments. The samples were measured in air atmosphere from 30 to  $800^\circ\text{C}$ , with a heating rate of  $10^\circ\text{C min}^{-1}$ .

The morphology of the membranes was studied by scanning electron microscopy (SEM) on Nova Nano and Quanta 600 microscopes, using a voltage in the range of 3–5 kV and a working distance in the range of 3–10 mm. Before performing the measurements, the samples were coated with iridium using a Quorum Q150TES equipment. By using transmission electron microscopy (TEM) we studied the cross-section morphology of the membranes. Initially the membranes were embedded in Epoxy resin at  $60^\circ\text{C}$  and then ultrathin sections (70 nm) were cut using an ultramicrotome (Leica EM UC6). The membranes were stained with phosphotungstic acid before performing the measurements using a FEI Tecnai 12 microscope operating at 120 kV.

The solvent resistance of the membranes was evaluated with UV spectrophotometer (NanoDrop 2000c) using equation (1), following a procedure described in [26]:

$$\text{Solvent resistance \%} = 100 (1 - A_1/A_0) \quad (1)$$

where  $A_0$  and  $A_1$  are the absorbance of solutions which contain unmodified and crosslinked membranes, respectively.

The contact angle measurement was performed by using Kruss EasyDrop equipment and the values were defined as the average of 6 measurements.

Mechanical measurements were performed with TA Instruments Q800 Dynamic Mechanical Analyzer in tensile mode. Rectangular samples (15x5 mm) were cut from the membranes with 70–80  $\mu\text{m}$  thickness. The stress-strain behavior was recorded using a force ramp of 0.1 N/m, at 25  $^{\circ}\text{C}$ , until break. Five samples were tested for each membrane. The ultimate tensile properties are calculated as the average of stress and strain at break. Strain–recovery analysis was performed by subjecting membranes to a stress of 0.5 MPa for 20 min, followed by a recovery period of 80 min with removed stress. The applied stress level was chosen to ensure that the creep measurements remained in the linear viscoelastic deformation regime of stress-strain curves and it matches the 5 bar pressure used for flux measurements. A small preload force of 0.01 N was applied to keep the sample right in the recovery regime.

The membrane performances were measured using a dead-end cell, at a pressure of 5 bar achieved with nitrogen. The filtration area of the membranes was 0.95  $\text{cm}^2$ . The solvent permeance was measured for 3 h and was evaluated using equation (2):

$$J = Q/A\Delta P \quad (2)$$

where  $Q$  is the permeation rate ( $\text{L h}^{-1}$ ),  $A$  is the effective filtration area ( $\text{m}^2$ ), and  $\Delta P$  is the pressure difference (bar).

The membrane rejection was measured by filtration of a mixture of polystyrene (PS) oligomers (2, 3, 10, 20 and 30  $\text{kg mol}^{-1}$ ) dissolved in THF and poly(ethylene glycol) (PEG) (3  $\text{kg mol}^{-1}$ ) dissolved in DMF.

The concentrations of the feed solutions were 1  $\text{mg ml}^{-1}$  of PS in THF and 2  $\text{mg ml}^{-1}$  of PEG in DMF. The membranes were conditioned by permeating pure solvents for 3 h before the

sieving experiments. Sieving experiments were conducted for 1 h, then the permeate samples were collected for subsequent analysis. The rejection (R) was evaluated using equation (3):

$$R(\%) = 100 (1 - C_p/C_f) \quad (3)$$

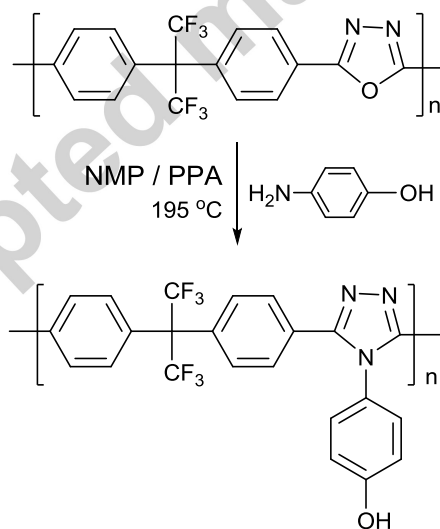
where  $C_p$  is the solute concentration in the permeate and  $C_f$  is the solute concentration in the feed. Gel permeation chromatography (GPC) was used to analyze the permeate samples and the feed. One GPC system was equipped with an Agilent refractive index detector and DMF was used as a mobile phase at 45°C. Another GPC system was equipped with a Viscotek employing a GPCmax module and a GPC-TDA 305 system and THF was used as a mobile phase at 35°C. For both GPC systems we used polystyrene standards for calibration.

### 3. Results and discussion

#### 3.1. Synthesis of polytriazole (PTA-OH) and crosslinked polytriazole membranes

Scheme 1 shows the synthesis procedure for polytriazole with OH groups. The polytriazole was prepared by reaction of polyoxadiazole precursor with 4-aminophenol at high temperature. The reaction took place by nucleophilic attack of amino groups on the oxadiazole ring, resulting in the corresponding 4-substituted 1,2,4-triazole by thermal treatment [29]. High conversion of oxadiazole in triazole rings can be achieved by simply adding to the reaction mixture small amounts of polyphosphoric acid (PPA). For this system, 0.04 g of PPA per gram of polyoxadiazole is sufficient to obtain a 95–98% conversion of oxadiazole into triazole rings in 10–15 h at 195°C. The PTA-OH has good solubility in polar solvents such as DMF, DMAc, DMSO and NMP, which confer a great advantage in membranes processing and manufacturing. The good solubility is due to the combination of the high number of grafted polar OH groups and aromatic rings, and the presence of hexafluoroisopropylidene units [30]. We investigated the

structure of the PTA-OH by using NMR. Fig. 1 shows the  $^1\text{H}$ -NMR and  $^{13}\text{C}$ -NMR of polytriazole. The presence of new grafted OH groups is confirmed by the chemical shift at 10.45 ppm, and the presence of new grafted aromatic ring is confirmed by the chemical shift at 7.00 ppm. The small chemical shift at around 8.3 ppm is associated with residual oxadiazole rings. The strong chemical shift at 154.3 ppm in  $^{13}\text{C}$ -NMR spectra confirms the formation of triazole rings. The grafted aromatic ring and OH groups are associated with the chemical shifts at 116.9 and 159.7 ppm, respectively. The absence of chemical shift at 164 ppm, which is characteristic of oxadiazole rings [26], demonstrates that all oxadiazole was converted to triazole rings. To quantify the conversion of this reaction, we divided the integrated areas of the chemical shift at 7.00 ppm, which is associated with triazole rings, by the integrated areas of chemical shift at 8.36 ppm, which is associated with oxadiazole rings. We obtained 98% conversion.



**Scheme 1.** Synthesis of polytriazole (PTA-OH).

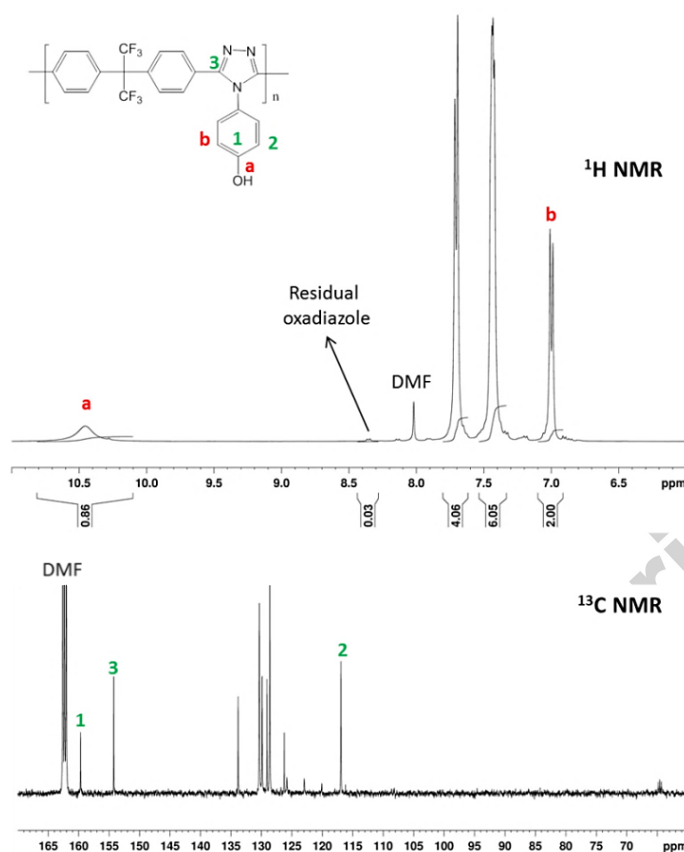
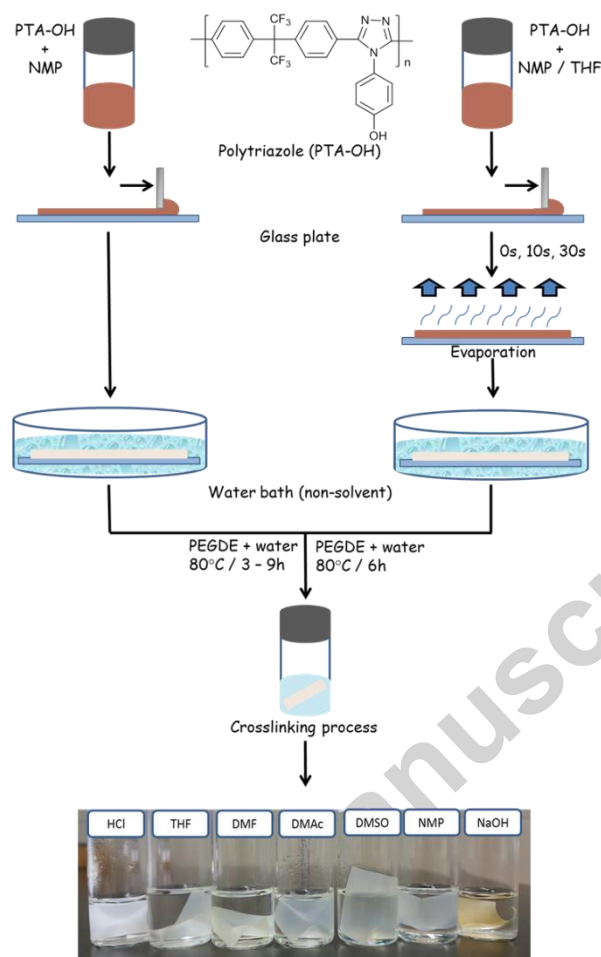


**Fig. 1.**  $^1\text{H}$  NMR and  $^{13}\text{C}$  NMR of PTA-OH.

Crosslinked polytriazole membranes were synthesized by exposing the porous membranes, immediately after formation by phase inversion, to PEGDE in water at  $80^\circ\text{C}$ , following the procedure presented in Scheme 2. PEGDE was chosen as crosslinker due to its low cost, non-toxicity and high solubility in water [31, 32]. With that we consider the crosslinking reaction a green process, which is an important advantage for the membrane industry, considering that most reported crosslinked OSN membranes are obtained by using more harmful crosslinkers (diamine or dihalogenates derivats) or organic solvents (acetonitrile or n-heptane) [11,16,17]. Another advantage of using PEGDE as a crosslinker is that it can act as a pores preservation agent [33]. The porous membranes were cast using 18 wt % polymer solutions in NMP or 9/1 NMP/THF.



**Scheme 2.** Preparation of crosslinked membranes; photograph of membranes crosslinked for 6 h and immersed in different organic solvents for 6 months.

The membranes obtained from the solution in NMP were exposed to the crosslinker for 0, 3, 6 and 9 h. The membranes obtained from the solution in NMP/THF were exposed to crosslinker for 6 h, but before immersion in water the casting solution was evaporated for 0, 10 and 30 s. To demonstrate the high stability of the crosslinked membranes in harsh environment, we immersed the membrane modified for 6h in THF, DMF, DMAc, DMSO, NMP and acid and base solutions for 6 months (Scheme 2). Only slight swelling occurs in the case of DMF, DMAc, DMSO and NMP and no change or swelling was observed in THF after 6 month. Using equation 1, we quantified the stability of the membrane immersed in DMF, and it is 99.5%.

FTIR and TGA were used to follow the crosslinking reaction at different times (Fig. 2). Fig. 2a shows the FTIR spectra for membranes obtained from solutions in NMP. The presence of new peaks in the spectra at  $2870 - 2928\text{ cm}^{-1}$ , which is characteristic for aliphatic C–H stretching vibration from PEGDE [34], and at  $1090\text{ cm}^{-1}$ , which is characteristic for the ether groups of PEGDE, prove that the crosslinking reaction was successful. The intensity and the broadness of the peak at  $1090\text{ cm}^{-1}$  is similar for the membranes crosslinked for 6h and 9h, suggesting that the amount of incorporated PEG segment is also similar. The peak at  $1518\text{ cm}^{-1}$  is characteristic of triazole rings [35]. Fig. 2b shows the TGA curves for the same membranes. The membrane without crosslinking has only one degradation stage, which starts at  $450^{\circ}\text{C}$  and is associated with polymer degradation, while the crosslinked membranes have two degradation stages, which start at  $230^{\circ}\text{C}$  and  $450^{\circ}\text{C}$  which are associated with the crosslinker and polymer degradation, respectively. The weight loss of the first degradation stage can be associated with the total amount of PEG segment in the membranes. The weight loss slightly increased from 28% to 31% when the reaction time increased from 3 h to 6 h, while no significant additional weight loss was observed when the reaction time increased from 6 h to 9 h. By increasing the reaction time, the number of active group decreases, while the polymer chains become more rigid and the mobility of the chains decrease. From FTIR and TGA results, it can be concluded that the maximum degree of crosslinking was achieved after 6 h of reaction and the maximum amount of PEG segment incorporated during the crosslinking reaction was 31%. Table 1 shows the water contact angle measured for unmodified and crosslinked membranes. The contact angle decrease from  $74^{\circ}$  to around  $60^{\circ}$ , indicating that after crosslinking the membranes become more hydrophilic.

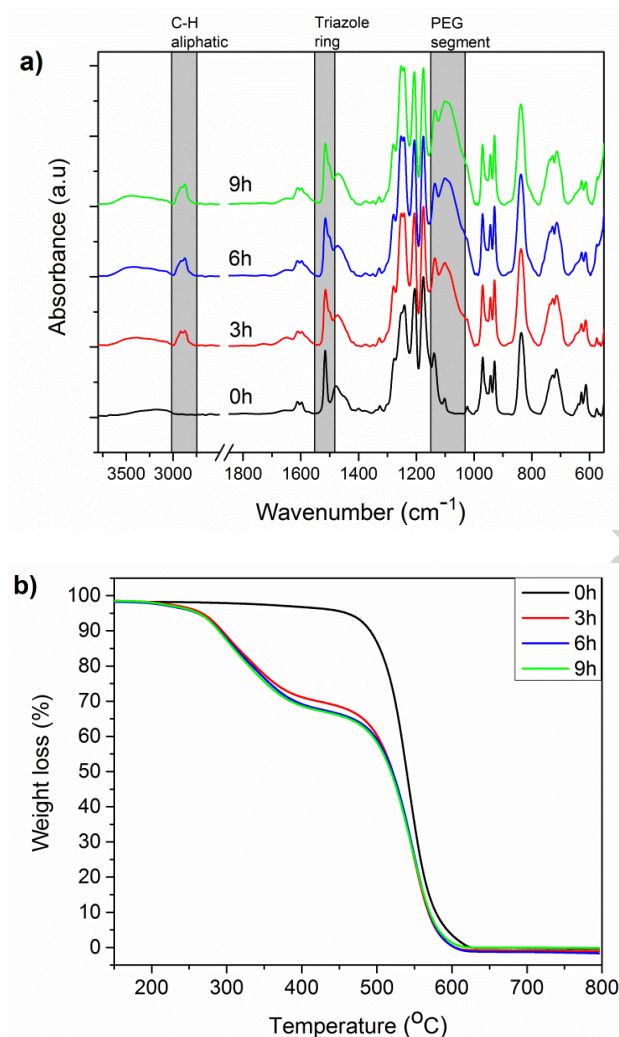


**Fig. 2.** (a) FTIR spectra and (b) TGA curves for membranes prepared from 18 wt% PTA-OH solutions in NMP, exposed to PEGDE crosslinker for different times.

### 3.2. Mechanical properties of polytriazole membranes

High mechanical stability is important, specially for pressure driven membrane applications, to assure that at high applied pressure the plastic deformation would be minimal and the membrane performance would maintain for long time [36]. Creep, time dependent deformation, could be detrimental under working conditions and finally could lead to membrane



failure. We investigated the effect of PEG segment on the mechanical properties of crosslinked membranes.

Tensile strength and Young's modulus were determined from stress-strain experiments. All the membranes exhibited similar stress-strain behavior, typical of glassy polymers. Application of load initially caused a linear increase of strain due to elastic response of the membranes, followed by a plastic deformation until the break point. The Young's modulus, calculated as the slope of stress-strain curve in the elastic region, together with the tensile strength and elongation at break are listed in Table 1. The Young's modulus of the crosslinked membranes is slightly higher than that of the unmodified membrane, while the elongation at break slightly decreased.

From the creep and recovery curves, obtained with the application and removal of load, different regions can be observed, as reported in Fig. 3. Firstly, an instantaneous increase of strain occurs, due to the stretching of polymeric chains. This is followed by the viscoelastic response, involving time-dependent molecular rearrangements. At the end of the load application period, viscous flow is observed. Once the stress is released, a certain portion of creep is instantaneously recovered, followed by a gradual strain recovery due to the visco-plastic nature of the material. The recovery period involves time-dependent molecular relaxations as the polymer attempts to regain the original dimensions. When the polymers experience viscous flow, creep strain remains in the polymer as a permanent deformation. As it can be observed in Fig. 3, if compared with the pristine membrane, the crosslinked membranes have less pronounced creep, which implies that the crosslinks restrict molecular rearrangements and improve the membrane deformation resistance of membranes. The strain values at the end of the loading period were reduced by 19%, 28% and 31% for the membranes crosslinked for 3 h, 6 h and 9 h, respectively.

For these membranes the elastic deformation is decreased and, in addition, the viscoelastic response is described by flatter curves. Thus, the membrane durability under mechanical stress is improved.

**Table 1.** Water contact angle and Stress-strain data of porous membranes prepared from 18 wt% PTA-OH solutions in NMP, exposed to the crosslinker for different times.

Crosslinking Time (h)	Contact angle (°)	Young's Modulus (MPa)	Tensile Strength (MPa)	Elongation at Break (%)
0	$74 \pm 2$	$101 \pm 3$	$4.3 \pm 0.1$	$12 \pm 1$
3	$67 \pm 1$	$106 \pm 5$	$4.5 \pm 0.4$	$11 \pm 2$
6	$61 \pm 1$	$117 \pm 3$	$4.5 \pm 0.5$	$9 \pm 2$
9	$58 \pm 2$	$117 \pm 4$	$4.5 \pm 0.4$	$9 \pm 2$

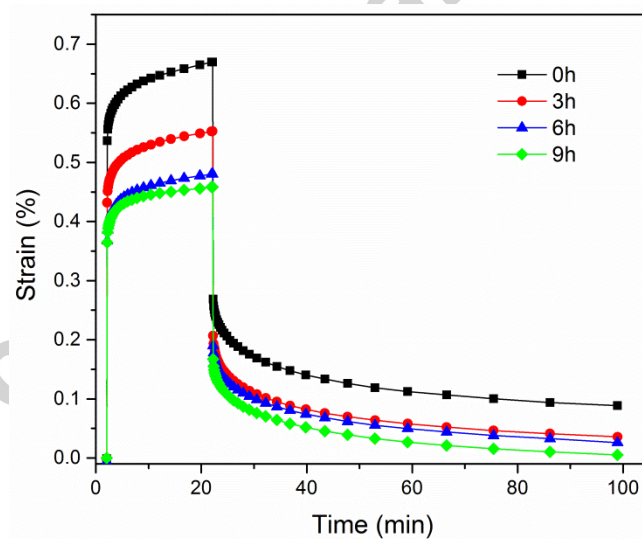


**Fig. 3.** Creep – recovery curves for membranes prepared from 18 wt% PTA-OH in NMP, exposed to crosslinker for different times.

To describe the creep component, we used the four element model of Maxwell and Kevin-Voigt (spring and dashpot in series with a parallel combination of spring and dashpot). The

overall deformation is the sum of three components - instantaneous elastic deformation, delayed elastic deformation and Newtonian flow – and is given by the equation (4):

$$\varepsilon = \frac{\sigma_0}{E_1} + \frac{\sigma_0}{E_2} \left(1 - e^{-\frac{t}{\tau}}\right) + \frac{\sigma_0}{\eta_1} t \quad (4)$$

where  $\varepsilon$  is the strain or deformation,  $\sigma_0$  is the applied stress,  $t$  is the time after loading,  $E_1$  and  $\eta_1$  are the modulus and viscosity of Maxwell spring and dashpot and  $\tau = \eta_2/E_2$  is the retardation time that is the time required for the Voigt element to deform to 63.21% (or  $1-1/e$ ) of its total deformation [37]. The parameter  $E_1$  was calculated from the instantaneous creep strain,  $\eta_1$  and  $E_2$  were estimated from the slope and from the intercept of the time-dependent deformation in the region of equilibrium flow, while the retardation time from the exponential portion of the viscoelastic response,  $E_2$ , was calculated from  $\tau = \eta_2/E_2$  and their values are summarized in Table 2. In agreement with stress–strain results, the values  $E_1$  indicate that the elasticity of crosslinked membranes was improved. The increase of the delayed elasticity  $E_2$ , related with the stiffness, suggests a reinforcement of crosslinked membranes. The retardation time is increased for these membranes, indicating more solid-like behavior. The increased values of viscosity  $\eta_1$  translate into reduced flow and the permanent deformation is less pronounced for the crosslinked membranes. According to these observations, the crosslinking increases the membranes resistance to deformation. By incorporating the PEG segment as crosslinker an enhancement of Young's modulus, better creep resistance and less permanent deformation were achieved.

**Table 2.** Creep parameters calculated with the four element model and the permanent strain after recovery for membranes prepared from solutions in NMP exposed to crosslinker for different times.

Crosslinking	$E_1$ (MPa)	$\eta_1$ (MPa·s)	$E_2$ (MPa)	$\eta_2$ (MPa·s)	$\tau$ (s)	Permanent
--------------	-------------	------------------	-------------	------------------	------------	-----------

Time (h)						strain (%)
0	93	12972	572	498	87.0	0.09
3	116	17123	581	570	98.1	0.04
6	136	20117	599	581	96.9	0.03
9	137	28531	685	609	88.9	0.01

### 3.3. Membrane morphology

SEM was used to investigate the morphology of the membranes before and after crosslinking. Fig. 4 shows the SEM images of membranes prepared from solution in NMP. The size of the membrane pores are reduced by increasing the crosslinking reaction time, showing that after 6 hours exposure to crosslinker the pores are practically filled or covered by the PEG segments. The cross-sectional morphology of the membranes before and after crosslinking prepared in NMP was investigated by TEM (Fig. 5). For the membrane crosslinked during 6 h, pores are not seen near the surface, while a structured morphology is observed for the uncrosslinked membrane. Furthermore, phosphotungstic acid preferentially stains the PEG richer phases, which constitute the dark areas in Fig. 5b. Therefore, we assumed that the highly contrasted thin layer on the top of the membranes and the spherical aggregates on the walls of the finger-like cavities could be associated with the PEG segments.

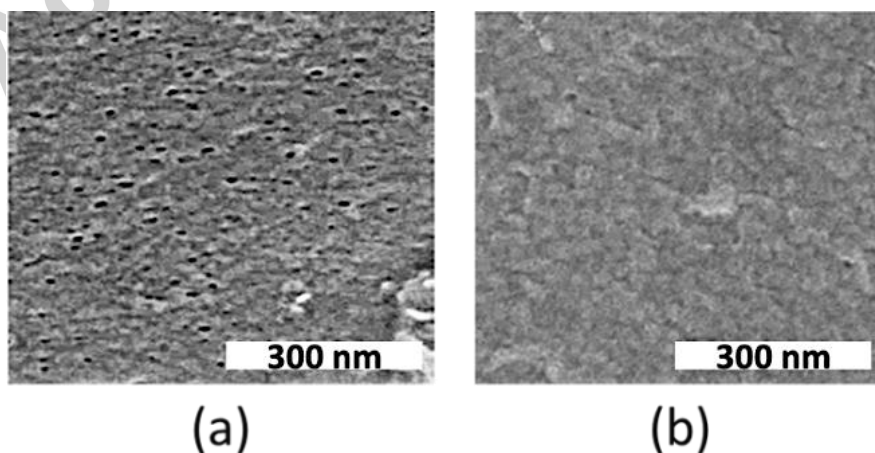


**Fig. 4.** SEM images of PTA-OH membranes prepared from solutions in NMP, (a) without crosslinking and (b) with 6 hours exposure to crosslinker.

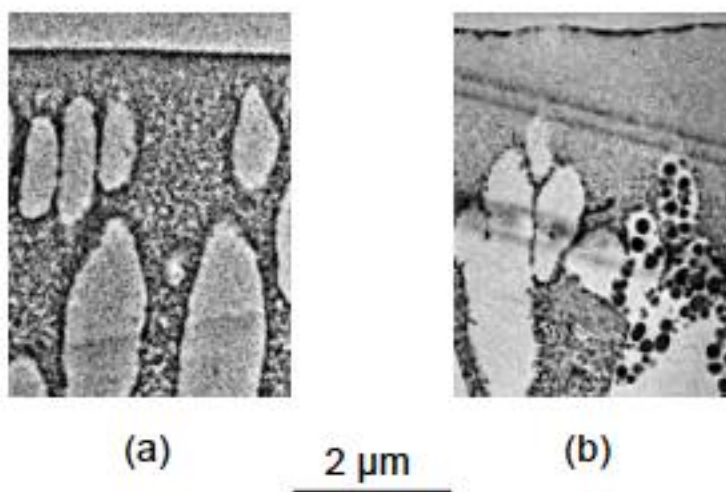


**Fig. 5.** TEM images of PTA-OH membranes prepared from solutions in NMP, (a) without crosslinking and (b) with 6 hours exposure to crosslinker and stained with phosphotungstic acid.

### 3.4. Filtration performance of crosslinked polytriazole membranes

We measured the polytriazole membranes permeation for water, DMF and THF. The rejection of polystyrene oligomers dissolved THF was measured in dead-end cell under pressure of 5 bar. Table 3 shows the performance of membranes prepared from solutions in NMP. The unmodified membrane has higher water permeance than the crosslinked membranes, demonstrating that after crosslinking the pores size decreases. For all crosslinked membranes the highest solvent permeance was measured for THF, which is the solvent with the lowest viscosity (0.47 mPa s). The viscosity of DMF is 0.92 mPa s. The DMF permeance for the membranes crosslinked with PEGDE was up to  $22 \text{ L m}^{-2} \text{ h}^{-1} \text{ bar}^{-1}$  with MWCO  $7 \text{ kg mol}^{-1}$ . This is almost 4 times higher than what we previously obtained for membranes, with comparable MWCO, by

crosslinking copolyazole membranes with (3-glycidyloxypropyl)trimethoxysilane (Table 5) [26]. With PEGDE we were able to have lower MWCO, down to 3 kg mol<sup>-1</sup>, with 8.5 L m<sup>-2</sup> h<sup>-1</sup> bar<sup>-1</sup> permeance.

**Table 3.** Performance of membranes prepared from solutions in NMP, exposed to crosslinker for different times.

Cross-linking Time (h)	Permeance of pure solvents (L m <sup>-2</sup> h <sup>-1</sup> bar <sup>-1</sup> )			Permeance of THF/PS (L m <sup>-2</sup> h <sup>-1</sup> bar <sup>-1</sup> )	MWCO (kg mol <sup>-1</sup> )
	Water	DMF	THF		
0	140 ± 30	-	-	-	-
3	13 ± 3	13 ± 0.1	31 ± 8	23 ± 5	10
6	21 ± 5	22 ± 6	49 ± 7	27 ± 5	7
9	25 ± 5	20 ± 6	44 ± 10	30 ± 2	8

Fig. 6a shows the DMF permeance for 10 h, for crosslinked membrane prepared from solution in NMP as a function of time. The DMF permeance is constant after the first 15 minutes, showing the high stability of the membranes in the solvents and indicating that no significant physical aging and compaction appears during the measurement. These results are consistent with the creep-recovery analysis, which demonstrated that the presence of a flexible crosslinker enhances the membrane mechanical stability. For polyimide XP84 (the most common polymeric materials in OSN applications), 60% permeance decline was reported when tested in methanol after the first 4 hours of filtration [36]. Compared to that value, the polytriazole membranes are more stable. To confirm the robustness of the polytriazole membranes, the DMF flux was measured by varying pressure from 3.2 to 9.5 bar (Fig. 6b). The good linearity indicates that the polytriazole membranes have a constant permeable area, which does not collapse under increasing pressure [36].

The resistances of the crosslinked membranes in organic solvents and in low pH were then tested after immersing the membranes up to 6 months in DMAc or in HCl. Fig. 6c shows the DMF permeance for the crosslinked membranes after the long time exposure. For both cases (immersion in HCl or DMAc), the DMF permeance is constant and similar to the permeance obtained before the exposure (Table 4). This indicates that the crosslinked polytriazole membranes are robust and membrane performance would maintain for long time.

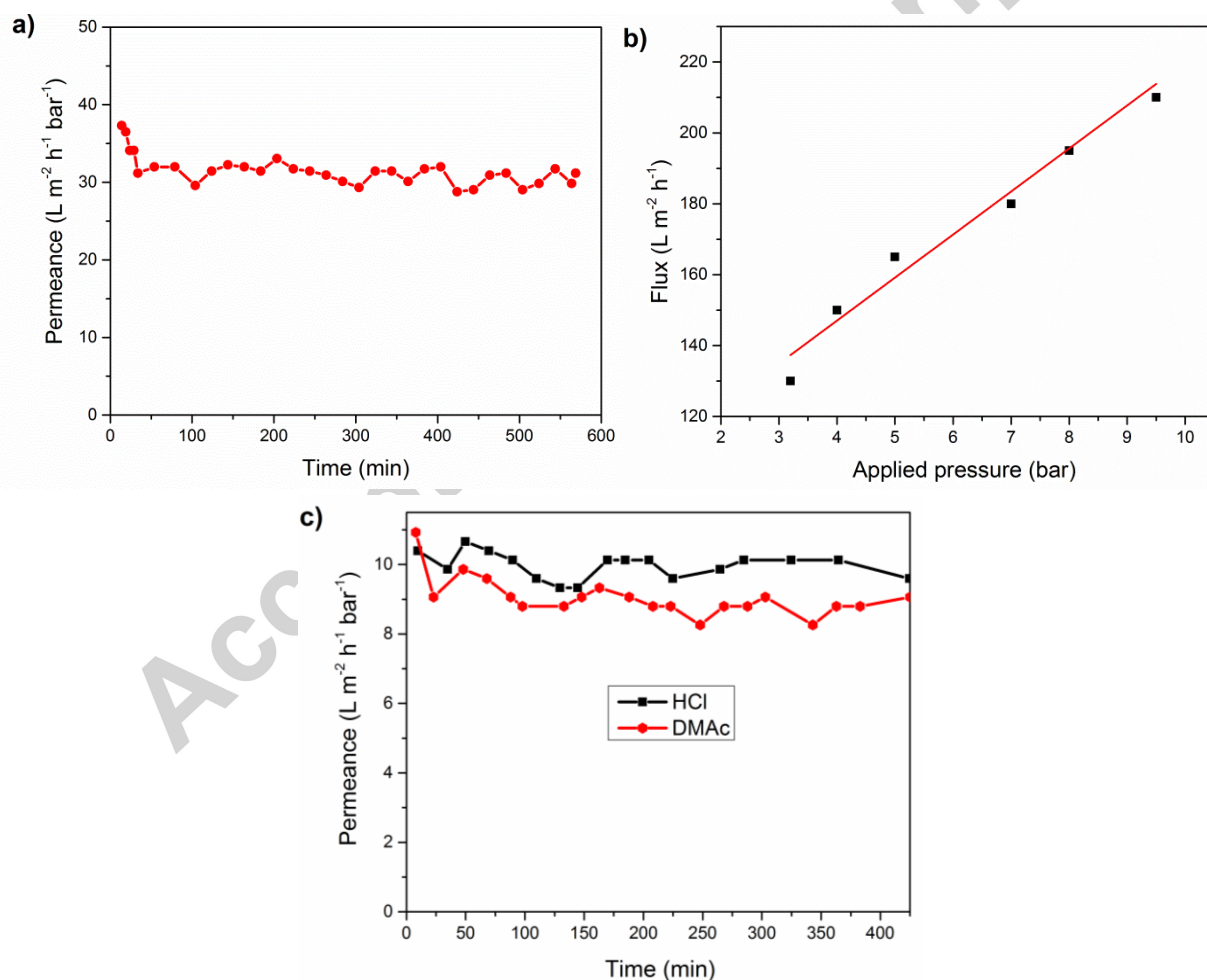


**Fig. 6.** (a) DMF permeance as a function of time and (b) variation of DMF flux with pressure for membranes prepared from NMP solution and exposed for 6 hours to crosslinker; (c) DMF

permeance with time for the membranes prepared from NMP/THF (10s evaporation), crosslinked during 6 hours and immersed in 1M HCl solution or in DMAc for 6 months.

The molecular weight cut-off (MWCO) values for membranes prepared from solutions in NMP were obtained by identifying the minimum molecular weight with 90% rejection (Fig. 7a) [35]. The MWCO values are in the range of 7 – 10 kg mol<sup>-1</sup>, corresponding to solutes with hydrodynamic radii in the range of 2.3 – 2.8 nm [39]. Thus, the membranes have a MWCO at the lower UF range. By comparing the results in terms of solvents flux and rejection, we can conclude that 6 h of crosslinking leads to the best membrane filtration performance.

In an attempt to decrease even more the pores size in the NF range, we used a mixture of 9/1 NMP/THF to dissolve the polytriazole and to cast the membranes. By adding a volatile co-solvent, such as THF, a denser skin layer is obtained during the evaporation step [13]. The membranes performance are shown in Table 4.

**Table 4.** Performance of membranes obtained from solutions in NMP/THF with different evaporation times and 6 hours exposure to crosslinker.

Evaporation Time (s)	Permeance of pure solvent (L m <sup>-2</sup> h <sup>-1</sup> bar <sup>-1</sup> )		Permeance of solvent/solute (L m <sup>-2</sup> h <sup>-1</sup> bar <sup>-1</sup> )		MWCO (kg mol <sup>-1</sup> )	
	DMF	THF	DMF/PEG	THF/PS	DMF	THF
0	12 ± 2	18 ± 3		18 ± 5	-	8
10	9 ± 1	18 ± 2	8.0 ± 0.5	14 ± 1	3	3
30	8.4 ± 0.5	21 ± 3		20 ± 2	-	7

Different evaporation times varying from 0 to 30 s led to different MWCO values. The minimum value was obtained with 10 s evaporation. The MWCO was in this case 3 kg mol<sup>-1</sup> (Figure 7b). The hydrodynamic radii corresponding to this MWCO value is 1.5 nm. For the same membrane, we measured the retention of PS in THF and PEG in DMF (Fig.



**8). Similar results were obtained. This membrane has a MWCO at the upper end of the NF range.** The solvent permeance obtained with membranes prepared from solutions in NMP/THF is slightly lower. The THF permeance is in the range of  $18 - 21 \text{ L m}^{-2} \text{ h}^{-1} \text{ bar}^{-1}$ , compared to  $22 \text{ L m}^{-2} \text{ h}^{-1} \text{ bar}^{-1}$  for those prepared from solutions in NMP.

This demonstrates that by using different casting solutions and different crosslinking times, it is possible to adjust the membrane pore size to obtain a MWCO that covers the entire limit between the UF range and the NF range. The performances of the crosslinked polytriazole membranes in terms of solvent permeance and solute rejection are comparable with the performance of other membranes reported in the literature, such as copolyazole, polybenzimidazole, mixed matrix or nanocellulose membranes [6,7,40]. The performances of those membranes are listed in Table 5.

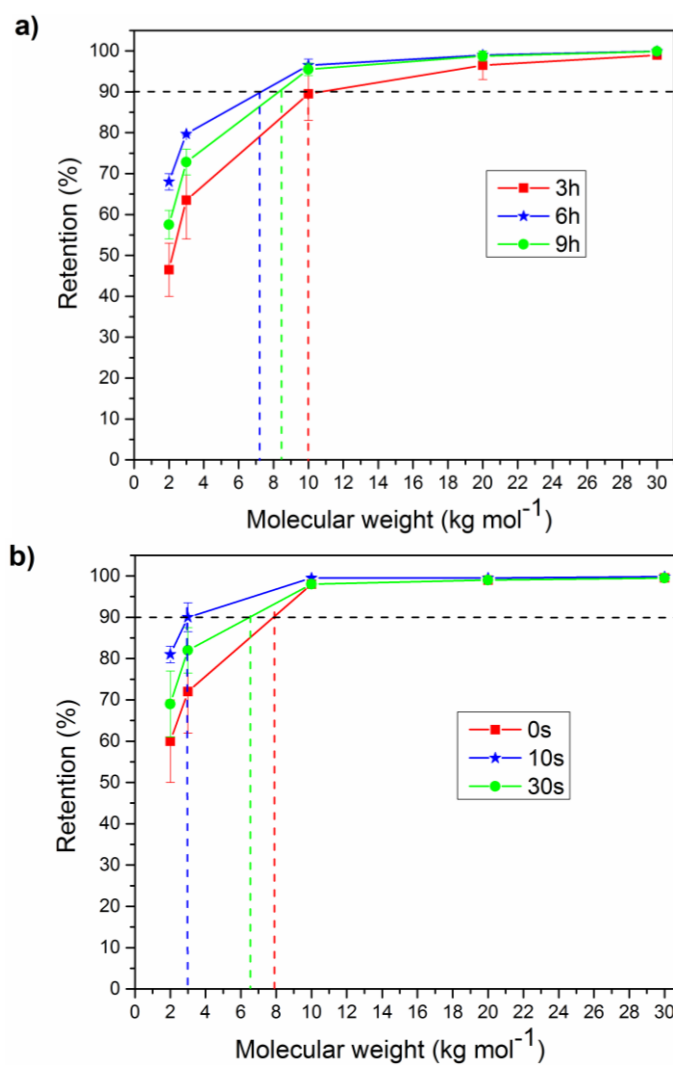


**Fig. 7.** Retention of PS in THF as a function of molecular weight for membranes prepared from solutions in (a) NMP and (b) NMP/THF.

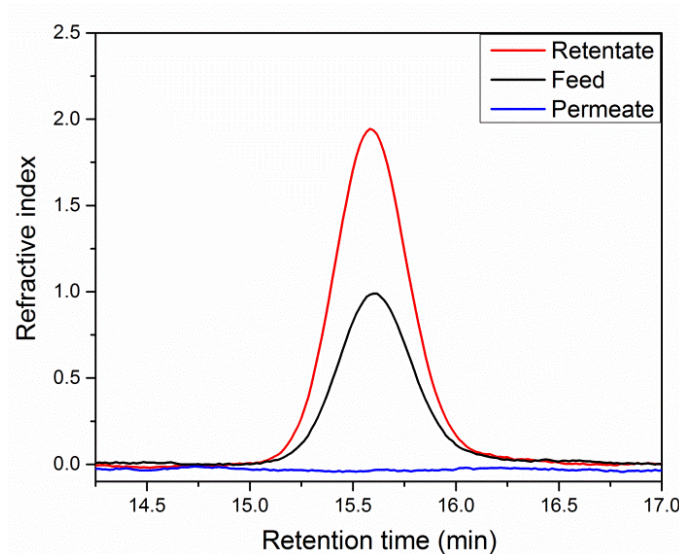


**Fig. 8.** Retention of PEG ( $3 \text{ kg mol}^{-1}$ ) in DMF for membrane prepared from solutions in NMP/THF, and evaporated for 10s.

**Table 5.** Summary of performance of different membrane materials

Membrane material	Solvent	Permeance ( $\text{L m}^{-2} \text{ h}^{-1} \text{ bar}^{-1}$ )	Solute	Solute MW ( $\text{kg mol}^{-1}$ )	MWCO
<b>Copolyazole (CPA)</b> [26]	THF	40	PS	10 – 150	22
	DMF	6.5			
<b>Polyoxadiazole (POD)</b> [20]	THF	200 – 240	PS	10 - 300	60
<b>Polybenzimidazole (PBI)</b> [16]	acetonitrile	17 – 37	PEG	0.4 – 8	2
	DMF	1 – 7			
<b>MOF HKUST-1</b> [6, 7]	acetone	15	PS	0.236 -1.8	1.8

## Conclusions

We prepared crosslinked membranes for organophilic filtration from a new polytriazole 98% functionalized with free OH groups and crosslinked with poly(ethylene glycol) diglycidyl ether (PEGDE). The OH-functionalized polymer was synthesized by reacting a polyoxadiazole precursor with aminophenol. The reaction takes place with 98% conversion of oxadiazole to OH-functionalized triazole rings. The resulting crosslinked membranes are stable in a wide range of

organic solvents. Creep-recovery analysis highlighted the role of the crosslinking in enhancing the membrane mechanical stability. The crosslinked membranes have high creep recovery with lower permanent deformation, indicating that by using a flexible crosslinker such as PEGDE we can obtain membranes, which are stable in several organic solvents, without losing their flexibility. The best membrane performance in terms of solvent flux and solute retention was achieved for the membranes exposed 6 hours to the crosslinker. By using different casting solutions and different crosslinking times it is possible to tailor the MWCO, corresponding to the lower ultrafiltration range to upper end nanofiltration, suitable for a wide range of applications.

### Acknowledgements

This research was supported by King Abdullah University of Science and Technology (KAUST).

### References

- [1] P. Vandezande, L. E. M. Gevers, I. F. J. Vankelecom, Solvent resistant nanofiltration: separating on a molecular level, *Chem. Soc. Rev.* 37 (2008) 365 – 405.
- [2] P. Marchetti, M.F. Jimenez Solomon, G. Szekely, A.G. Livingston, Molecular separation with organic solvent nanofiltration: A critical review, *Chem. Rev.* 114 (2014) 10735–10806.
- [3] V. Freger, Outperforming nature's membranes, *Science* 348 (2015) 1317 – 1318.
- [4] B. Van der Bruggen, Fundamentals of membrane solvent separation and pervaporation, in *Membrane Operations: Innovative Separations and Transformations*, ed. E. Drioli and L. Giorno, Wiley-VCH Verlag GmbH&Co.KGaA, Weinheim, 2009, pp.45–61.

- [5] Y. Li, T. Verbiest, R. Strobbe, I.F.J. Vankelecom, Improving the performance of pervaporation membranes via localized heating through incorporation of silver nanoparticles, *J. Mater. Chem. A* 1 (2013) 15031 – 15038.
- [6] J. Campbell, G. Szekely, R.P. Davies, D.C. Braddock, A.G. Livingston, Fabrication of hybrid polymer/metal organic framework membranes: mixed matrix membranes versus in situ growth, *J. Mater. Chem. A* 2 (2014) 9260–9271.
- [7] J. Campbell, R.P. Davies, D.C. Braddock, A.G. Livingston, Improving the permeance of hybrid polymer/metal–organic framework (MOF) membranes for organic solvent nanofiltration (OSN) – development of MOF thin films via interfacial synthesis, *J. Mater. Chem. A* 3 (2015) 9668 – 9674.
- [8] L.H. Wee, Y. Li, K. Zhang, P. Davit, S. Bordiga, J. Jiang, I.F.J. Vankelecom, J.A. Martens, Submicrometer-sized ZIF-71 filled organophilic membranes for improved bioethanol recovery: mechanistic insights by Monte Carlo simulation and FTIR spectroscopy, *Adv. Funct. Mater.* 25 (2015) 516 – 525.
- [9] S. Sorribas, P. Gorgojo, C. Tellez, J. Corona, A.G. Livingston, High flux thin film nanocomposite membranes based on metal–organic frameworks for organic solvent nanofiltration, *J. Am. Chem. Soc.* 135 (2013) 15201 – 15208.
- [10] Y. Li, L.H. Wee, A. Volodin, J.A. Martens, I.F.J. Vankelecom, Polymer supported ZIF-8 membranes prepared via an interfacial synthesis method, *Chem. Commun.* 51 (2015) 918 – 920.
- [11] K. Vanherck, G. Koeckelberghs, I.F.J. Vankelecom, Crosslinking polyimides for membrane applications: A review, *Prog. Polym. Sci.* 38 (2013) 874 – 896.

- [12] M. Liu, G. Yao, Q. Cheng, M. Ma, S. Yu, C. Gao, Acid stable thin-film composite membrane for nanofiltration prepared from naphthalene-1,3,6-trisulfonylchloride (NTSC) and piperazine (PIP), *J. Membr. Sci.* 415–416 (2012) 122 – 131.
- [13] A. K. Holda, B. Aernouts, W. Saeys, I.F.J. Vankelecom, Study of polymer concentration and evaporation time as phase inversion parameters for polysulfone-based SRNF membranes, *J. Membr. Sci.* 442 (2013) 196 – 205.
- [14] D. Bhanushali, S. Kloos, C. Kurth, D. Bhattacharyya, Performance of solvent-resistant membranes for non-aqueous systems: solvent permeation results and modeling, *J. Membr. Sci.* 189 (2001) 1 – 21.
- [15] V. Smuleac, J.Wu, S. Nemser, S. Majumdar, D. Bhattacharyya, Novel perfluorinated polymer-based pervaporation membranes for the separation of solvent/water mixtures, *J. Membr. Sci.* 352 (2010) 41 – 49.
- [16] I.B. Valtcheva, S.C. Kumbharkar, J.F. Kim, Y. Bhole, A.G. Livingston, Beyond polyimide: Crosslinked polybenzimidazole membranes for organic solvent nanofiltration (OSN) in harsh environments, *J. Membr. Sci.* 457 (2014) 62 – 72.
- [17] D.Y. Xing, S.Y. Chan, T.S. Chung, The ionic liquid [EMIM]OAc as a solvent to fabricate stable polybenzimidazole membranes for organic solvent nanofiltration, *Green Chem.* 16 (2014) 1383 – 1392.
- [18] J. da Silva Burgal, L.G. Peeva, S. Kumbharkar, A.G. Livingston, Organic solvent resistant poly(ether-ether-ketone) nanofiltration membranes, *J. Membr. Sci.* 479 (2015) 105 – 116.

- [19] J. da Silva, Bursal, L. Peeva, A.G. Livingston, Towards improved membrane production: using low-toxicity solvents for the preparation of PEEK nanofiltration membranes, *Green Chem.* 18 (2016) 2374-2384.
- [20] H. Maab, S.P. Nunes, Porous polyoxadiazole membranes for harsh environment, *J. Membr. Sci.* 445 (2013) 127 – 134.
- [21] S. H. Han, N. Misdan, S. Kim, C. M. Doherty, A. J. Hill, Y. M. Lee, Thermally Rearranged (TR) Polybenzoxazole: Effects of Diverse Imidization Routes on Physical Properties and Gas Transport Behaviors, *Macromolecules* 43 (2010), 7657-7667.
- [22] S. Kim, Y. M. Lee, Highly proton-conductive thermally rearranged polybenzoxazole for medium-temperature and low-humidity polymer electrolyte fuel cells, *J. Power Sources* 247 (2014) 286-293.
- [23] D. Gomes, S.P. Nunes, Fluorinated polyoxadiazole for high-temperature polymer electrolyte membrane fuel cells, *J. Membr. Sci.* 321 (2008) 114 – 122.
- [24] D. Gomes, R. Marschall, S. P. Nunes, M. Wark, Development of polyoxadiazole nanocomposites for high temperature polymer electrolyte membrane fuel cells, *J. Membr. Sci.* 322 (2008) 406 – 415.
- [25] M. L. Ponce, J. Roeder, D. Gomes, S. P. Nunes, Stability of sulfonated polytriazole and polyoxadiazole membranes, *Asia-Pac. J. Chem. Eng.* 5 (2010) 235-241.
- [26] S. Chisca, P.H.H. Duong, A.-H. Emwas, R. Sougrat, S.P. Nunes, Crosslinked copolyazoles with a zwitterionic structure for organic solvent resistant membranes, *Polym. Chem.* 6 (2015) 543 – 554.
- [27] S. Loeb, S. Sourirajan, Seawater demineralisation by means of an osmotic membrane, *Adv. Chem. Ser.* 38 (1962) 117 – 132.

- [28] S. P. Nunes and K. V. Peinemann, *Membrane Technology in the Chemical Industry*, Wiley, 2nd edn, 2006.
- [29] A. Moulin, M. Bibian, A.L. Blayo, S. El Hannouni, J. Martinez, J.A. Fehrentz, Synthesis of 3,4,5-Trisubstituted-1,2,4-triazoles, *Chem. Rev.* 110 (2010) 1809 – 1827.
- [30] I. Sava, S. Chisca, A. Wolinska-Grabczyk, A. Jankowski, M. Sava, E Grabiec, M. Bruma, Synthesis and thermal, mechanical and gas permeation properties of aromatic polyimides containing different linkage groups, *Polym. Int.* 64 (2015) 154–164.
- [31] N. Vasylieva, B. Barnych, A. Meiller, C. Maucier, L. Pollegioni, J-S. Lina, D. Barbier, S. Marinesco, Covalent enzyme immobilization by poly(ethylene glycol) diglycidyl ether (PEGDE) for microelectrode biosensor preparation, *Biosens. Bioelectron.*, 36 (2011) 3993–4000.
- [32] S. Quan, S. Li, Z. Wang, X. Yan, Z. Guo, L. Shao, A bio-inspired CO<sub>2</sub>-philic network membrane for enhanced sustainable gas separation, *J. Mater. Chem. A* 3 (2015) 13758 – 13766.
- [33] H. Siddique, Y. Bhole, L.G. Peeva, A.G. Livingston, Pore preserving crosslinkers for polyimide OSN membranes, *J. Membr. Sci.* 465 (2014) 138–150.
- [34] S. Chisca, I. Sava, M. Bruma, Porous polyimide films obtained by using lithium chloride as pore-forming agent, *Polym. Int.* 62 (2013) 1634 – 1643.
- [35] K-L Wang, T-Y Tseng, H-L Tsai, S-C Wu, Resistive switching polymer materials based on poly(aryl ether)s containing triphenylamine and 1,2,4-triazole moieties, *J. Polym. Sci: Part A: Polym. Chem.* 46 (2008) 6861 – 6871.
- [36] S. Karan, Z. Jiang, A.G. Livingston, Sub-10 nm polyamide nanofilms with ultrafast solvent transport for molecular separation, *Science* 348 (2015) 1347–1351.



- [37] K.P. Menard, *Dynamical Mechanical Analysis - A Practical Introduction*, CRC Press, 1999.
- [38] Y.H. See Toh, X.X. Loh, K. Li, A. Bismarck, A.G. Livingston, In search of a standard method for the characterisation of organic solvent nanofiltration membranes, *J. Membr. Sci.* 291 (2007) 120–125.
- [39] E. Uliyanchenko, P.J. Schoenmakers, S. van der Wal, Fast and efficient size-based separations of polymers using ultra-high-pressure liquid chromatography, *J. Chromatogr. A* 1218 (2011) 1509–1518.
- [40] A. Mautner, K.-Y. Lee, P. Lahtinen, M. Hakalahti, T. Tammelin, K. Li, A. Bismarck, Nanopapers for organic solvent nanofiltration, *Chem. Commun.* 50 (2014) 5778-5781.

## Highlights

- New crosslinked polytriazole membrane for organophilic filtration
- High stability in wide range of solvents was obtained using poly (ethylene glycol) diglycidyl ether as crosslinker.
- High creep recovery with lower permanent deformation.
- No significant physical aging and compaction appears during the solvent permeance.